High-Precision Motion Detection Using Low-Complexity Doppler Radar With Digital Post-Distortion Technique

Changzhan Gu, *Member, IEEE*, Zhengyu Peng, *Student Member, IEEE*, and Changzhi Li, *Senior Member, IEEE*

Abstract—Owing to the low complexity and high level of system integration, the quadrature direct-conversion architecture is widely used in Doppler radar for noncontact detection of slow periodic motions such as mechanical vibrations and physiological motions of respiration and heartbeat. However, precise detection of the complete motion pattern has been challenging due to the high-pass characteristics of the ac-coupled baseband circuitry. A few techniques have been proposed to preserve the actual motion pattern in radar sensing based on hardware modifications that add system complexity and cost. In this paper, a digital post-distortion (DPoD) technique is proposed to compensate for the signal distortions in the digital baseband domain. Without any cumbersome hardware modification, the complete pattern of slow periodic motions can be detected using a simple quadrature direct-conversion architecture with ac-coupled baseband. Experimental results show that the proposed Doppler radar with the DPoD technique is robust to compensate signal distortions and can be used for precise detection of slow Doppler motions (near dc) where ac coupling typically attenuates the signal.

Index Terms—Doppler radar, high precision, low complexity, motion detection, noncontact, quadrature.

I. INTRODUCTION

NONCONTACT detection based on radar technologies are attracting more and more research efforts within the microwave community due to the vast applications [1]–[7]. The continuous-wave Doppler radar has been widely used for noncontact detection of versatile periodic motions, such as vibration motions [8]–[10], and physiological activities [11]–[13]. For some applications, only the frequency information is desired, e.g., noncontact vital sign detection of respiration rate and heartbeat rate [12]. However, there are many situations where the complete motion pattern is important. For example, the thoracic wall displacement must be accurately detected in radar respiration monitoring to interpret the shallow breathing due to the

apnea events [14]; in motion-adaptive cancer radiotherapy, the complete respiration pattern needs to be preserved to indicate the tumor location [15]; structural health monitoring requires accurate amplitude information to assess the safety and health conditions of the infrastructures [16]. The precise detection of versatile periodic motions requires the radar system be able to preserve the complete signal pattern.

Among all the possible Doppler radar architectures, the quadrature direct-conversion architecture is perhaps the one that has been most widely used. Its popularity is due to the low architectural complexity, low hardware cost, and high level of system and chip integration [17]. Over the past few decades, researchers over the world have made tremendous efforts to promote Doppler radar research. Various techniques have been proposed on both the signal processing and the hardware to increase the robustness and the accuracy of radar motion detection [6], [7], [18], [19].

On the signal-processing side, small angle approximation was first introduced for quadrature radar so that either the in-phase (I) or quadrature (Q) channel can be used as the detected signal [18]. The arctangent demodulation was introduced to combine the I/Q signals to eliminate the null point problem and increase the linear region of phase demodulation [19]. Nevertheless, phase unwrapping may be necessary to avoid the phase discontinuity in arctangent demodulation [20]. An enhanced differentiate and cross-multiply (DACM) algorithm was employed to avoid phase unwrapping in quadrature radar phase demodulation [21]. Recently, a phase-demodulation approach was proposed to extend the linear phase demodulation region to a few wavelengths [22]. To deal with the hardware demerits, compensation methods based on radar measured data and ellipse fitting were proposed to eliminate the impact of I/Q imbalance [23], [24], and dc-offset estimation approaches were investigated for accurate demodulation [17], [25]. Baseband equalization techniques were proposed for pulse radar ranging or imaging [26], [27], or for preserving the signal pattern [28]. In recent years, continuous wave (CW) Doppler radar is becoming an attractive approach for accurate motion detection, where high-precision detection of the motion amplitude at a low hardware cost is of vital importance. The ac coupling is still an important problem that challenges the Doppler radar to achieve high accuracy in displacement detection. Few signal-processing techniques have been proposed to tackle the signal distortion problem in ac coupling to ensure high accuracy in radar motion detection.

This article has been accepted for inclusion in a future issue of this journal. Content is final as presented, with the exception of pagination.

2

IEEE TRANSACTIONS ON MICROWAVE THEORY AND TECHNIQUES

In the quadrature direct-conversion receiver, the backscattered signal received at the radar RF front-end is amplified and mixed with the local oscillator (LO) signal to be converted directly to baseband. Therefore, dc offset is inevitable [15], [19]. To remove the dc offset, ac coupling is usually used between the radar mixer output and the radar baseband amplifier. However, the high-pass characteristics of the ac-coupled signal chain may lead to significant signal distortions when measuring low-frequency motions [29]. This demerit prohibits the Doppler radar from precisely measuring the complete signal pattern of the target motions [15], [29]. Researchers have proposed a few techniques on the hardware side to avoid signal distortion and preserve the signal integrity. For example, several dc-coupled receiver architectures have been proposed to calibrate the dc offset while preserving the dc information [15], [19]. The dc-coupled receiver has all-pass characteristics that avoid the distortion to low-frequency motions or slow motions with stationary moment. However, the dc-coupled structure requires extra effort of dc tuning and also adds to hardware complexity. Another approach to avoid signal distortion is to use the digital IF architecture. Instead of directly converting the RF signal down to baseband, the receiver digitizes the radar received signal at IF, thus avoiding the ac-coupled baseband structure [30], [31]. However, the IF architecture requires cumbersome hardware design and a high-speed digitizer, which increases both the system complexity and hardware cost.

In this paper, a post-distortion technique is proposed to compensate for the signal distortion caused by ac coupling in Doppler radar sensing. The proposed post-distortion technique is performed in the digital domain and does not require any hardware modification. The ac-coupled Doppler radar system can use a simple quardature direct-conversion architecture to measure low-frequency motions without losing information on motion pattern. In contrast to the pre-distortion technique, which is widely used in power amplifiers' linearization, the proposed digital post-distortion (DPoD) technique applies signal compensation in the digital baseband to recover the signal information that is lost in an ac-coupled receiver. The DPoD technique "linearizes" the high-pass characteristics of ac-coupling so that the ac-coupled baseband performs virtual "all-pass" characteristics to the input signals. Therefore, without requiring any hardware modifications, signal integrity can be largely preserved using the conventional low-cost ac-coupled radar hardware.

II. THEORY

A. Signal Distortion

Fig. 1(a) shows the block diagram of the 2.4-GHz quadrature direct-conversion radar system. In Doppler radar motion detection, a single-tone RF signal is transmitted to the moving target, which backscatters the RF signal to the radar receiver. According to the Doppler theory, the backscattered signal has motion information modulated in the phase. The RF signal received at the radar front-end is amplified, filtered, and directly
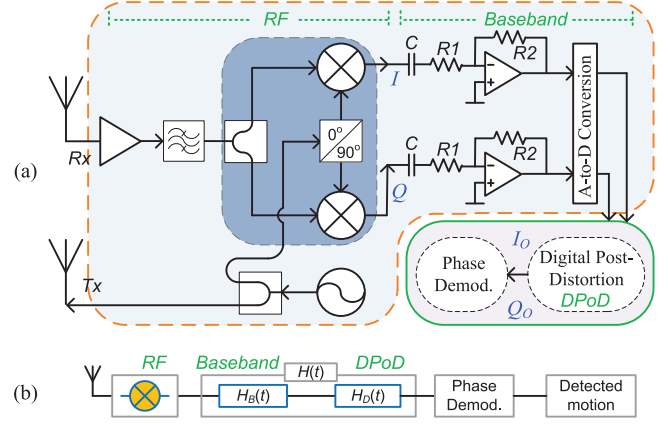

Fig. 1. (a) Block diagram of the 2.4-GHz quadrature direct-conversion Doppler radar with DPoD technique. Baseband is ac coupled to remove dc offset. (b) Simplified diagram showing baseband response of $H_B(t)$, DPoD response of $H_D(t)$, and the complete system response of $H(t)$.

converted to baseband I/Q signals using a quadrature mixer. The mixer output I/Q signals are [24]

$$I(t) = A \cdot \cos\left(\frac{4\pi x(t)}{\lambda} + \frac{4\pi d_0}{\lambda} + \Delta\theta(t)\right) + \mathrm{DC}_I \quad (1)$$

$$Q(t) = A \cdot (1 + \Delta\varepsilon) \cdot \sin\left(\frac{4\pi x(t)}{\lambda} + \frac{4\pi d_0}{\lambda}\right.$$
$$\left. + \Delta\theta(t) + \Delta\sigma\right) + \mathrm{DC}_Q \quad (2)$$

where A is the amplitude, $x(t)$ is the time-varying relative displacement of the subject, λ is the wavelength of the carrier signal, d_0 is the nominal distance from radar to the subject, $\Delta\theta(t)$ is residual phase noise including the constant phase shift, $\Delta\varepsilon$ is the amplitude imbalance factor, $\Delta\sigma$ is the phase error, and DC_I and DC_Q are dc offsets in I/Q channels.

Owing to the advancement of the integrated circuit (IC) technologies, today's mixers have good quadrature balance. For example, the quadrature mixer used in this work, i.e., Skyworks73009, has a maximum I/Q amplitude imbalance of 0.3 dB and a typical phase error of only $1°$. In case there is large quadrature imbalance, it can be compensated by methods such as the ellipse-fitting technique [24] and the data-based technique [23]. Therefore, the phase imbalance $\Delta\varepsilon$ and phase error $\Delta\sigma$ are not considered in this work. The mixer output I/Q signals can be rewritten as [9]

$$I(t) = A \cdot \cos\left(\frac{4\pi x(t)}{\lambda} + \Delta\phi(t)\right) + \mathrm{DC}_I$$
$$= A \cdot \sum_{n=-\infty}^{n=+\infty} J_n\left(\frac{4\pi m}{\lambda}\right)\cos(n\omega t + \Delta\phi(t)) + \mathrm{DC}_I \quad (3)$$

$$Q(t) = A \cdot \sin\left(\frac{4\pi x(t)}{\lambda} + \Delta\phi(t)\right) + \mathrm{DC}_Q$$
$$= A \cdot \sum_{n=-\infty}^{n=+\infty} J_n\left(\frac{4\pi m}{\lambda}\right)\sin(n\omega t + \Delta\phi(t)) + \mathrm{DC}_Q \quad (4)$$

This article has been accepted for inclusion in a future issue of this journal. Content is final as presented, with the exception of pagination.

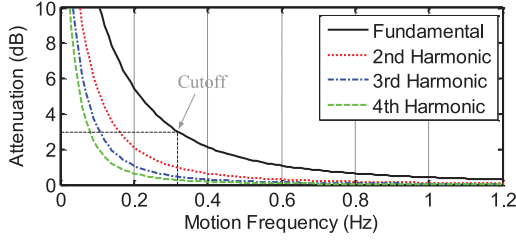GU *et al.*: HIGH-PRECISION MOTION DETECTION USING LOW-COMPLEXITY DOPPLER RADAR WITH DPoD TECHNIQUE 3

Fig. 2. Fundamental and harmonics from nonlinear phase modulation are subject to different degrees of attenuation at ac-coupled radar baseband.

Fig. 3. Simulated I/Q trajectory showing the error vector that is due to distortion at the ac-coupled baseband.

where $\Delta\phi(t) = 4\pi d_0/\lambda + \Delta\theta(t)$, $x(t) = m\sin(\omega t)$ is the target motion with amplitude of m and frequency of $\omega = 2\pi f$, $J_n(x)$ is the nth-order Bessel function of the first kind. It is seen from (3) and (4) that, due to the nonlinear phase modulation, the radar measured signal is not single tone, but has harmonics. Keeping the harmonic ratios is necessary for the signal integrity [29].

In order to reduce the impact of the quantization noise in analog-to-digital conversion, the mixer output I/Q signals are usually further boosted by the baseband amplifiers. Between the mixer output and the input of the baseband amplifier, ac coupling is widely used to deal with the dc offsets DC_I and DC_Q, which may saturate the baseband amplifiers, as shown in Fig. 1. The capacitor and the operational amplifier of the baseband form a first-order high-pass filter with cutoff frequency of $\omega_c = 1/(C \cdot R_1)$. It is known that, while measuring slow motions, signal distortion may happen if the harmonic ratios are changed when the target frequency and its harmonics are subject to different degrees of attenuation in the baseband high-pass filter [29]. Fig. 2 shows the attenuations for the fundamental tone and the harmonics at the ac-coupled baseband with $C = 10\,\mu\text{F}$ and $R1 = 50\,\text{k}\Omega$. It is seen that, at low motion frequency, the fundamental is subject to higher attenuation than the harmonics, which changes the harmonic ratios and leads to signal distortion. The lower the motion frequency, the higher attenuation the fundamental suffers from. The difference in attenuation decreases as the motion frequency increases. When the motion frequency is way beyond the cutoff frequency, e.g., 1.0 Hz, the fundamental and harmonics tend to endure the same degree of attenuation, which means no signal distortion.

B. Error Vector Magnitude

After dc-offset calibration, the I/Q signals shown in (3) and (4) are expected to form an ideal arch that fits with the circle with the radius of $[DC_I, DC_Q]$ centered in A in the I/Q plane [19]. The dc-offset calibration is necessary for accurate phase demodulation to recover the motion information [32]. However, due to the loss of the inherent harmonic ratios in ac coupling, the I/Q signals are distorted so that they no longer display an ideal arch, but exhibit a ribbon-like trajectory, as shown in Fig. 3. The ribbon-like trajectory makes it a challenging task to accurately calibrate the dc offsets and find the correct center $[DC_I, DC_Q]$, which may lead to inaccurate phase demodulation.

The error vector magnitude (EVM) is proposed as a measure of the degree of distortion and the quality of the I/Q trajectory. Without signal distortion, all the I/Q points are expected to ideally fall on the unit circle. However, with signal distortion, the
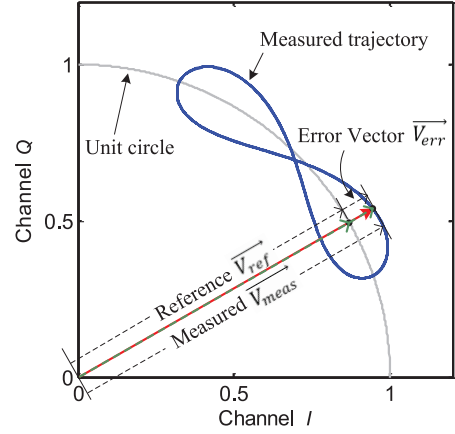
I/Q points may deviate from the unit circle with a vector of $\overrightarrow{V_{\text{meas}}}$, as shown in Fig. 3. The reference vector $\overrightarrow{V_{\text{ref}}}$ is defined as the vector from the center to the intersection between the unit circle and $\overrightarrow{V_{\text{meas}}}$. The error vector is then the difference between $\overrightarrow{V_{\text{meas}}}$ and $\overrightarrow{V_{\text{ref}}}$, i.e., $\overrightarrow{V_{\text{err}}} = \overrightarrow{V_{\text{meas}}} - \overrightarrow{V_{\text{ref}}}$. The EVM for the whole I/Q trajectory is defined as

$$\text{EVM (dB)} = \frac{\sum_{k=1}^{N} 10 \cdot \log_{10}\left(\frac{\left|\overrightarrow{V_{\text{err}}^k}\right|}{\left|\overrightarrow{V_{\text{ref}}^k}\right|}\right)}{N} \qquad (5)$$

where N is the number of signal points in the I/Q trajectory, V_{meas}^k is the vector from the circle center to the kth measured signal point, and V_{ref}^k is the kth reference vector from the center to the ideal circle. In order to accurately detect the subject's motion, the EVM must be minimized so that the I/Q trajectory could better represent the precise phase information caused by the target movement rather than the circuit imperfections. The EVM is not only determined by the signal to noise ratio, but also by the deviation from the trajectory to the unit circle. For frequency-fixed motions, as the motion magnitude increases the ribbon shape tends to expand so that the EVM worsens.

C. Distortion Compensation

The complex signal at the mixer output combing (3) and (4) is $C_{\text{in}}(t) = I(t) + j \cdot Q(t)$. The total system response between the mixer output and the phase demodulation algorithm is $H(t)$, which includes the baseband transfer function $H_B(t)$ and the DPoD transfer function $H_D(t)$, as shown in Fig. 1(b). The complex signal before phase demodulation is $C_o(t) = I_o(t) + j \cdot Q_o(t)$, as shown in Fig. 1(a). Without DPoD, the system response $H(t)$ attributes only to the analog baseband, i.e., $H(t) = H_B(t)$. $C_o(t)$ can be represented as the convolution of $C_{\text{in}}(t)$ and $H_B(t)$

$$C_o{}'(t) = I_o{}'(t) + j \cdot Q_o{}'(t) = C_{\text{in}}(t) * H_B(t) \qquad (6)$$

where $C_o{}'(t)$, $I_o{}'(t)$, and $Q_o{}'(t)$ represented the signals without DPoD. The signals are digitized to discrete-time signals $C_o{}'(n)$ by the analog-to-digital converter. Applying the

This article has been accepted for inclusion in a future issue of this journal. Content is final as presented, with the exception of pagination.

4   IEEE TRANSACTIONS ON MICROWAVE THEORY AND TECHNIQUES
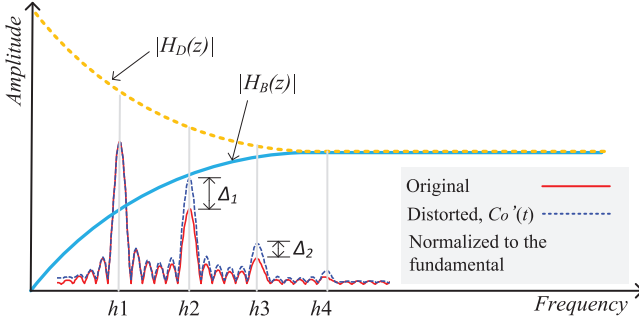

Fig. 4. Signal distortion is due to the change of harmonic ratios in ac-coupled baseband with high-pass characteristics of $|H_B(z)|$. The proposed DPoD technique employs a system response $|H_D(z)|$ in the digital domain to recover the harmonic ratios to compensate for the signal distortion.

z-transform to $C_o'(n)$ yields another representation in the z-domain,

$$C_o'(z) = C_{\text{in}}(z) \cdot H_B(z) \tag{7}$$

where $C_o'(z)$, $C_{\text{in}}(z)$, and $H_B(z)$ are the z-transforms of $C_o'(t)$, $C_{\text{in}}(t)$, and $H_B(t)$, respectively. The system response $H_B(z)$ representing the baseband circuit between the mixer output and the baseband amplifier can be expressed as

$$H_B(z) = A_s \cdot \frac{1 - \sum_1^M b_k \cdot z^{-k}}{1 - \sum_1^N a_k \cdot z^{-k}} \tag{8}$$

where A_s is the gain factor. The coefficients b_k/a_k determine the characteristics of the system response such as high pass or low pass that may cause distortion to the radar measured signal.

In the proposed DPoD technique, the signal distortion is compensated in the digital domain by an algorithm whose system response $H_D(z)$ is the inverse function of $H_B(z)$,

$$H_D(z) = \frac{1 - \sum_1^M a_k \cdot z^{-k}}{1 - \sum_1^N b_k \cdot z^{-k}}. \tag{9}$$

Fig. 4 shows the principle of the proposed DPoD technique. The second and third harmonics of the distorted signal are higher than those of the original signal. It is because they are subject to a less degree of distortion than the fundamental tone in the stopband of the baseband high-pass filter. By applying the compensation function $H_D(z)$, which adds more gain to the fundamental than the harmonics, the original harmonic ratios could be restored in the digital domain so as to avoid the distortion that happens in the analog domain. With DPoD, the system response $H(z)$ represents the transfer functions in both analog and digital domains. The recovered signal is

$$C_o'(z) \cdot H_D(z) = C_{\text{in}}(z) \cdot H_B(z) \cdot H_D(z) = A_s \cdot C_{\text{in}}(z). \tag{10}$$

As the radar measured motion information is modulated in the phase, the gain A_s has no contribution to the signal distortion. It is flat in the frequency domain, as the movement speed of up to a few Hz is much smaller than the bandwidth of the baseband
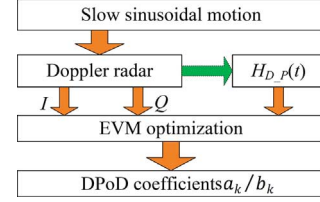

Fig. 5. Flowchart showing the procedure to obtain the DPoD coefficients.

amplifier of up to several MHz. The amplitude is calibrated out in arctangent demodulation [32].

The DPoD coefficients a_k/b_k can be obtained in hardware calibration by characterizing the baseband high-pass filter. The transfer function of the analog baseband is firstly determined according to the hardware structure. For example, the analog baseband in Fig. 1 has $C = 10~\mu\text{F}$ and $R1 = 50~\text{k}\Omega$. Thus, the baseband cutoff frequency is 0.32 Hz. The baseband is a first-order high-pass RC filter with coefficients $a_1 = 0.961$ and $b_1 = 1$. The baseband transfer function is then $H_B(z) = A_S \cdot [(1 - z^{-1})/(1 - 0.961 z^{-1})]$. The preliminary compensation function $H_{D\_P}(z)$ is then defined as the inversion of $H_B(z)$, i.e., $H_{D\_P}(z) = [(1 - 0.961 z^{-1})/(1 - z^{-1})]$. However, the coefficients may change due to the tolerance of the RC components in practical circuits. Fig. 5 shows a flowchart that illustrates the procedure to obtain the optimal DPoD coefficients. The Doppler radar is set up to measure a slow sinusoidal motion with frequency less than the cutoff frequency of the high-pass filter. The coefficients a_k/b_k are swept in a predefined range around the ideal values in $H_{D\_P}(z)$ so as to minimize the EVM of the I/Q trajectory. The coefficients a_k/b_k that achieve the best EVM are recorded as the DPoD coefficients. If the I/Q channels have different filter responses, DPoP with different coefficients could be applied to each channel individually. The frequency response of the fixed radar hardware is quite stable. Therefore, as long as the DPoD coefficients are properly calibrated, the radar with DPoD can accurately measure motions with different frequencies and patterns.

III. Simulation

A. DPoD Simulation

The first simulation is to demonstrate the theory of the proposed DPoD technique. A 0.25-Hz sinusoidal motion ($m = 1.7$ cm) is simulated and measured by a 2.4-GHz Doppler radar having the same architecture as Fig. 1 with $C = 10~\mu\text{F}$ and $R1 = 50~\text{k}\Omega$. If no DPoD is applied, which means that the total system response attributes solely to the baseband high-pass filter, the system response is $H(t) = H_B(t)$ and the simulation results are shown in Fig. 6(a). Without DPoD, the system response $H(t)$ shows high-pass characteristics. As the 0.25-Hz signal is less than the cutoff frequency of 0.32 Hz, the fundamental is located within the stopband of the high-pass filter. As seen in Fig. 6(a), the second and third harmonics of the distorted signal are higher than those of the original signal. It is because the fundamental and harmonics are subject to different degrees of attenuation, which changes the fundamental-to-harmonics ratios. The change of harmonic ratios leads to distorted I/Q trajectory shown as a ribbon-like shape [29]. The proposed DPoD

This article has been accepted for inclusion in a future issue of this journal. Content is final as presented, with the exception of pagination.

GU *et al.*: HIGH-PRECISION MOTION DETECTION USING LOW-COMPLEXITY DOPPLER RADAR WITH DPoD TECHNIQUE
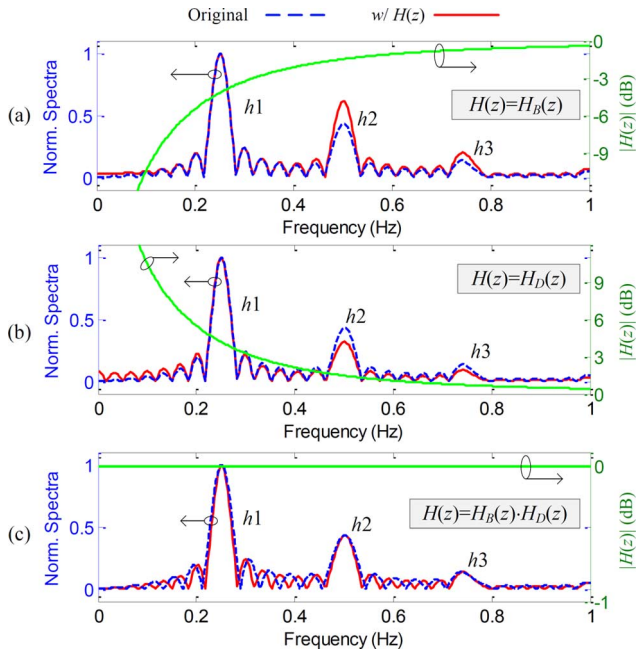
5

Fig. 6. Spectra of the simulation of radar measured 0.25-Hz sinusoidal motion when the total system response $H(t)$ is: (a) baseband response only $H_B(t)$, (b) DPD response only $H_D(t)$, and (c) combined system response $H_B(t) + H_D(t)$.
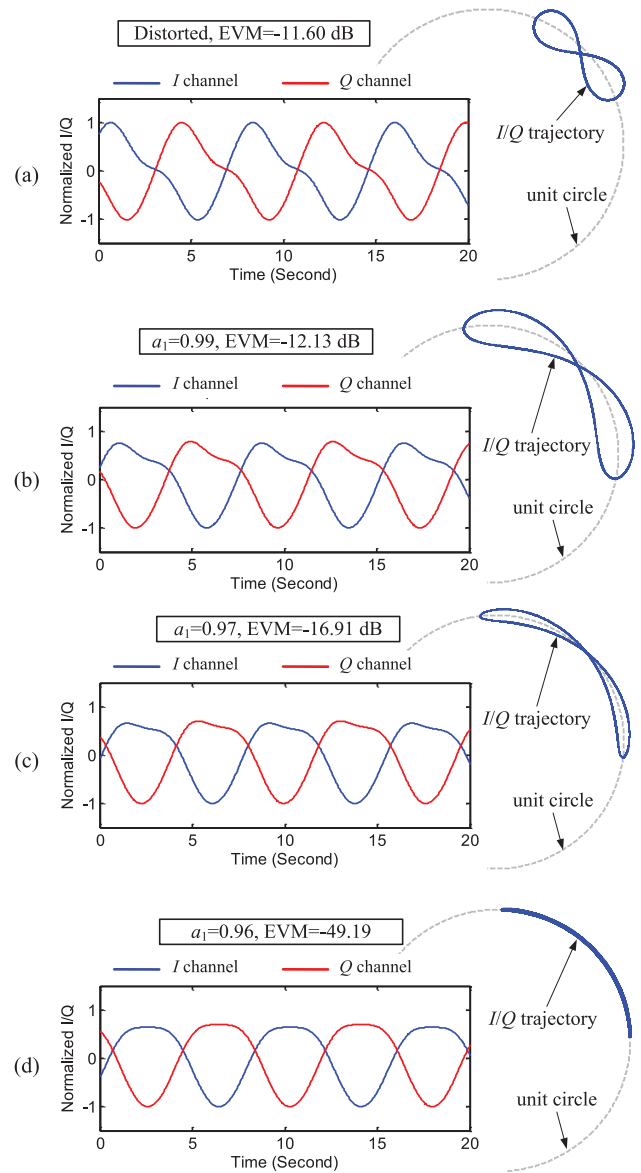

Fig. 7. Simulation results of distorted and compensated I/Q signals in time domain and in the I/Q plane: (a) distorted I/Q signals are showing ribbon-like I/Q trajectories. The distorted signals are compensated using different DPoD coefficients: (b) $a_1 = 0.99$, (c) $a_1 = 0.97$, and (d) $a_1 = 0.96$. The distortion is compensated and the I/Q trajectory is recovered to an ideal arch in (d).

technique works to smooth out the different attenuations to virtually increase the linearity of the baseband circuitry. It works in such a way that the DPoD response $H_D(t)$ is the inversion of the analog baseband response $H_B(t)$, which is shown in Fig. 6(b). Assuming that there is no signal distortion due to $H_B(t)$ and the total system response is only from DPoD, the simulation results are shown in Fig. 6(b). It is seen that the DPoD technique tends to change the harmonic ratios in an opposite way as compared with the ac-coupled baseband. If the DPoD technique is applied to the radar baseband, the combined system response would ideally be flat in the frequency domain, as shown in Fig. 6(c). It means that the fundamental and harmonics will suffer from the same degree of attenuation, which can be interpreted as the baseband insertion loss. Therefore, the Doppler radar would be able to retain the harmonic ratios to keep the signal integrity in motion detection. In practical radar systems, due to the $1/f$ noise in the amplifier and other hardware impairments that worsen near dc, the baseband response would be difficult to be equalized back to a flat frequency response. That being said, the harmonics of the target slow motion, e.g., respiration, may not be completely compensated to restore the inherent ratios. However, the proposed DPoD technique would help to greatly reduce the different degrees of attenuations suffered by different harmonics. In this way, the EVM could be improved for more accurate motion detection and the key information of a motion pattern could be preserved.

In the second simulation, the effectiveness of using the proposed DPoD technique to compensate signal distortions is evaluated. The simulated sinusoidal signal has a low frequency of 0.13 Hz ($m = 7.5$ mm). To simulate the distortion at ac-coupled baseband, the signal is filtered by a first-order high-pass RC filter with $C = 10$ μF and $R1 = 50$ kΩ, whose system response is

$H_B(z) = A_S \cdot [(1 - z^{-1})/(1 - 0.961z^{-1})]$. Fig. 7(a) shows the distorted I/Q signals in the time domain and the ribbon-like trajectory in the I/Q plane. The EVM of the distorted signal is -11.60 dB. In the simulation, a system response of $H_{D\_P}(z) = [(1 - a_1 \cdot z^{-1})/(1 - z^{-1})]$ is applied to the distorted signal to compensate the distortion. The coefficients a_1 is swept from 0.99 to 0.96. Fig. 7(b) shows the results after applying the compensation with $a_1 = 0.99$. Although the EVM is only improved by less than a dB, the ribbon-like shape tends to bend and acts more like an arch fitting with the circle. It is more obvious in Fig. 7(c), where $a_1 = 0.97$, that the ribbon shape tends to shrink and fits better with the unit circle. The EVM is now improved to -16.91 dB. When $a_1 = 0.96$ that is close to the actual coefficient 0.961 of the high-pass filter, the ribbon shape completely disappears and the I/Q trajectory is recovered to an ideal arch on

This article has been accepted for inclusion in a future issue of this journal. Content is final as presented, with the exception of pagination.

6   IEEE TRANSACTIONS ON MICROWAVE THEORY AND TECHNIQUES
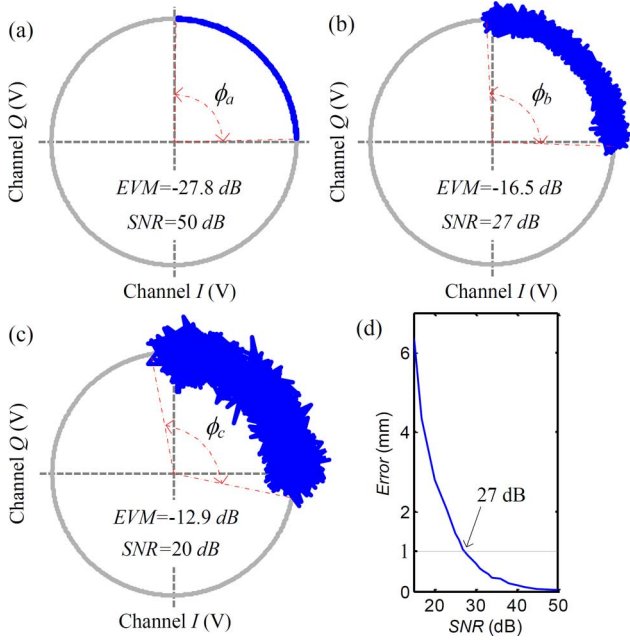

Fig. 8. Radian of the I/Q trajectory varies with SNR: (a) 50 dB, (b) 27 dB, and (c) 20 dB. (d) Noise in DPoD impacts the accuracy of radar measurement.
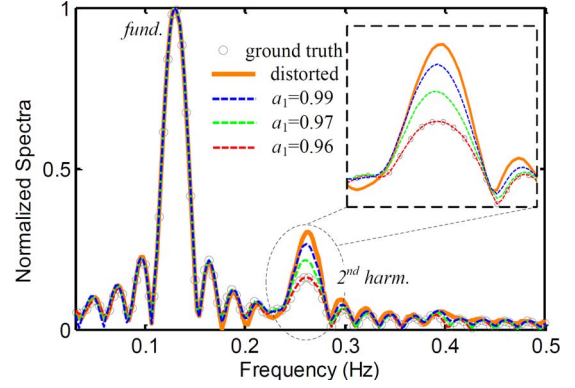

Fig. 9. Complex spectra of I/Q signals when the signals are distorted at ac-coupled baseband and compensated with different DPoD coefficients.

the unit circle with EVM of -49.19 dB, as shown in Fig. 7(d). It should be noted that the system noises and circuit imperfections are not considered in simulation. It would be difficult to have EVM near -50 dB in the real radar system. Empirically, EVM in the range of -20 to -30 dB is achievable and is good enough for a quality I/Q trajectory that can be used for accurate phase demodulation.

The distortion compensation can also be demonstrated in the frequency domain, as shown in Fig. 9. The ribbon-like I/Q trajectory is due to the loss of the intrinsic fundamental to harmonics ratios, i.e., the higher order harmonics suffer less attenuation as compared to the fundamental. In the real radar system, the second harmonic is the most important because: 1) its amplitude is not negligible compared to the fundamental and 2) the higher order harmonics, e.g., third and fourth order, are likely overwhelmed by the system noise. The DPoD compensation acts to adjust the harmonic amplitudes to restore the intrinsic harmonic ratios. As shown in Fig. 9, after applying DPoD with $a_1 = 0.96$, the harmonic amplitude is restored to the original, which means the distortion is compensated. It is also seen from Fig. 7 that the radian length of I/Q trajectory changes as a_1 approaches to the actual coefficient value. The radian of I/Q trajectory determines the displacement amplitude of the demodulated signal [32]. Therefore, the proposed DPoD technique is beneficial for optimizing the trajectory radian in distortion compensation for accurate displacement tracking.

B. Noise Analysis

The system noise has impact on the effectiveness of using DPoD for high-precision radar measurement. In the simulation, the same sinusoidal signal as in Fig. 7 (0.13 Hz, $m = 7.5$ mm) is contaminated with different noise levels and distorted by a first-order high-pass RC filter with $C = 10\,\mu$F and $R_1 = 50$ kΩ. A system response of $H_{D\_P}(z) = [(1 - 0.96 \cdot z^{-1})/(1 - z^{-1})]$

is then applied to the distorted signal to compensate for the distortion. As demonstrated in Fig. 7, without system noise, DPoD is able to recover the ideal I/Q trajectory with a fairly high EVM of -49.19 dB. Fig. 8 shows the simulation results with different noise levels. For 2.4-GHz radar, a sinusoidal motion with amplitude of 1/4 wavelength ($m = \lambda/4 = 31.25$ mm) occupies $360°$ on the I/Q graph [33]. The resolution is 31.25 mm$/360° = 0.087$ mm/degree. Therefore, without noise consideration, the I/Q trajectory of the simulated sinusoidal motion with $m = 7.5$ mm has a radian length of $86.4°$. It is seen in Fig. 8(a) that with a high SNR $= 50$ dB, the EVM is -27.8 dB and the trajectory radian ϕ_a of $86.7°$ is very close to the ideal radian of $86.4°$. The $0.3°$ radian difference leads to an error of only 0.03 mm. As signal-to-noise ratio (SNR) drops to 27 dB, as seen in Fig. 8(b), the EVM also decreases to -16.5 dB. Due to the impact of noise, the trajectory radian ϕ_b becomes $97.1°$, which corresponds to a measurement error of 0.9 mm. Higher noise level tends to further worsen both the EVM and the measurement accuracy, as can be seen from Fig. 8(c). The EVM is lowed to -12.9 dB and the trajectory radian ϕ_b is expanded to $117.6°$, which corresponds to an error of 2.7 mm. Fig. 8(d) shows the variation of radar measurement error with different SNR levels. It is seen that, to have sub-millimeter accuracy for a $m = 7.5$ mm sinusoidal motion, the SNR needs to be at least 27 dB.

IV. EXPERIMENTS

Experiments were carried out in a laboratory environment by using a 2.4-GHz ac-coupled Doppler radar sensor to measure periodic motions that include mechanical motions and the human respiration motions. Fig. 10 shows the experimental setup. The transmit power from the radar is 0 dBm, which is fed to the patch antenna having a gain of 5.8 dBi. The output I/Q signals are digitized by the data acquisition system (National Instruments USB-6009) with LabVIEW running in real time on the host laptop. The proposed DPoD technique was then applied to the recorded I/Q signals to compensate the potential signal distortions. The dc calibration method via compressed sensing was used to calibrate the dc offsets in I/Q signals [34]. For ac-coupled radar, the output of the baseband amplifier still has a dc-offset value because the amplifier itself
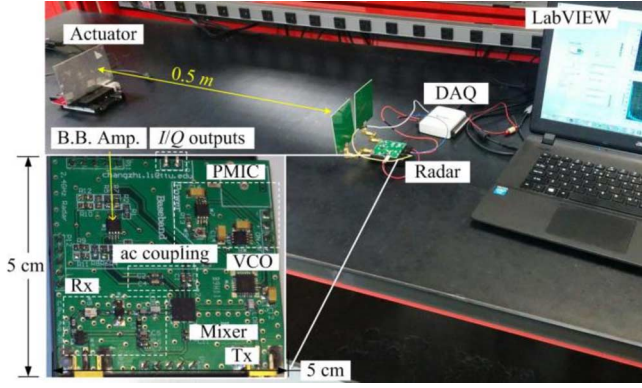
Fig. 10. Experimental setup using ac-coupled radar to measure mechanical motions.

should be properly dc biased. The calibration of dc information of the I/Q signals is important because the I/Q trajectory should be centered at (0,0) to fit the unit circle. The DACM algorithm was used to demodulate the motion information without phase discontinuity [21]. The radar sensor used in the experiments has the same architecture as Fig. 1 with a cutoff frequency of 0.32 Hz. The baseband acts as a first-order active high-pass filter. The DPoD coefficients were calibrated as $b_1 = 1$ and $a_1 = 0.955$. Therefore, the DPoD transfer function of $H_D(z) = [(1 - 0.955z^{-1})/(1 - z^{-1})]$ was employed in baseband signal processing to compensate the distortions.

A. Exp. 1: Slow Mechanical Motion

The ac-coupled Doppler radar was used to measure the mechanical movements of an actuator (Zaber T-NA08A50). As shown in Fig. 10, the actuator was placed about 0.5 m away from the Doppler radar and programmed to produce slow sinusoidal motions: the motion frequency is less than or close to the cutoff frequency of the high-pass filter. Two slow sinusoidal motions were measured by the Doppler radar: 1) $m = 4$ mm, $f = 0.17$ Hz and 2) $m = 6$ mm, $f = 0.32$ Hz. The experimental results are shown in Figs. 11–14.

As shown in Fig. 11(a), the slow sinusoidal motion was distorted at ac-coupled baseband and is showing a ribbon I/Q trajectory. However, the proposed DPoD technique effectively restored harmonic ratios to offset the distortion. Fig. 11(c) shows the spectral difference without and with DPoD. The recovered I/Q trajectory fits well with the unit circle, as shown in Fig. 11(b). The effectiveness of using DPoD in distortion compensation can also be seen from EVM, which is -18.07 dB for the distorted signals, but improved to -26.44 dB after using DPoD. The higher EVM means more accurate calibration of dc offsets, which results in more accurate phase demodulation. The demodulated signals of the slow motion with and without using DPoD are shown in Fig. 12. It is seen that the signal recovered by the proposed DPoD technique matches well with the ground truth that is the movement information programmed to the actuator. With DPoD, the measured displacement (*Disp. 1*) is 7.95 mm, which means the error is only 0.05 mm as compared to the ground truth of 8 mm. However, without DPoD, the measured displacement (*Disp. 2*) of 5.2 mm shows 1.8-mm deviation from the ground
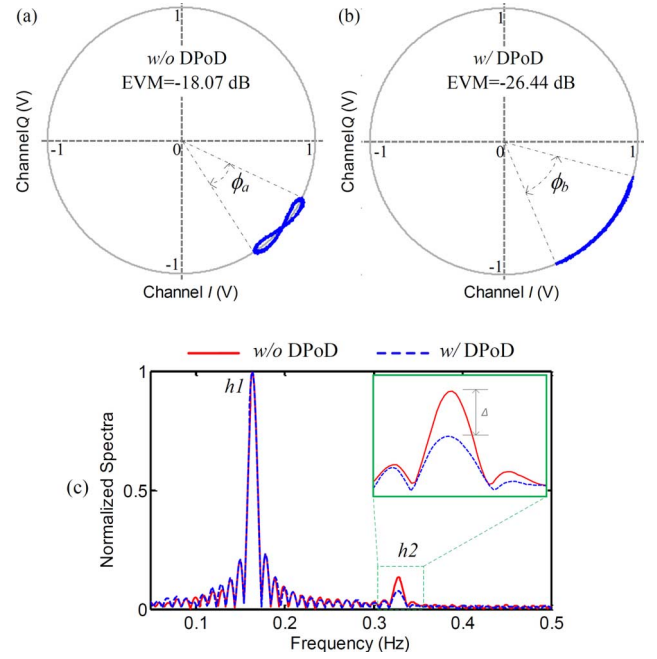

Fig. 11. I/Q trajectory of radar measured signals for a 0.17-Hz slow sinusoidal motion: (a) without DPoD, and (b) with DPoD. (c) Complex spectra combing I/Q signals without and with DPoD. The second harmonics show discrepancy.
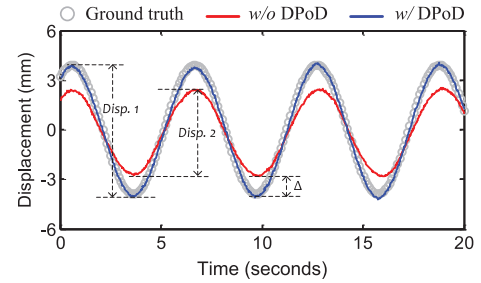

Fig. 12. Demodulated displacement signal of radar measured 0.17-Hz sinusoidal motion with and without DPoD is compared with the ground truth.

truth. The displacement difference can also be seen from the different trajectory radians of ϕ_a and ϕ_b. The radian of the I/Q trajectory, or the trajectory length, determines the magnitude of the demodulated displacement [32]. Without DPoD, I/Q signals are distorted so that the trajectory radian ϕ_a becomes smaller than the ideal one. With DPoD, the correct radian ϕ_b is recovered so that the phase demodulation is more accurate.

In the second slow motion, the motion frequency of 0.32 Hz is equal to the cutoff frequency of the ac-coupled high-pass filter. As seen in Fig. 2, even if the motion frequency sits at the cutoff point, the fundamental and the harmonics from nonlinear phase modulation are still subject to different degrees of attenuation. It is largely due to the low order of the high-pass filter, e.g., the filter in this work is first order, that the transition band is quite wide. As shown in Fig. 13(a), the ribbon I/Q trajectory means that the signal distortion may still happen even if the subject's motion is close to the cutoff frequency of the ac-coupled baseband. After applying the DPoD technique, the ribbon shape disappeared and the I/Q trajectory was recovered to an arch fitting well with the unit circle. The DPD technique also improved the EVM by 8 dB from -14.12 to -22.18 dB. The radian of the

This article has been accepted for inclusion in a future issue of this journal. Content is final as presented, with the exception of pagination.

8   IEEE TRANSACTIONS ON MICROWAVE THEORY AND TECHNIQUES
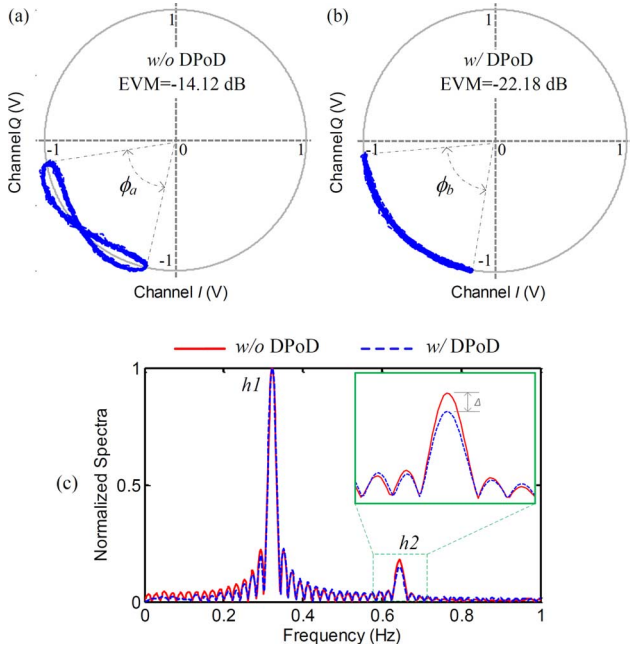

Fig. 13. I/Q trajectory of radar measured signals for a 0.32-Hz slow sinusoidal motion: (a) without DPoD, and (b) with DPoD. (c) Complex spectra combing I/Q signals without and with DPoD. The second harmonics show discrepancy.

Fig. 14. Demodulated displacement signal of radar measured 0.32-Hz sinusoidal motion with and without DPoD is compared with the ground truth.

I/Q trajectory in Fig. 12(a) is 63.9° and the radian with DPoD in Fig. 13(b) is 68.5°. The radian difference is less than that in Fig. 11 because the fundamental-to-harmonic ratio is less distorted as the motion frequency is closer to the cutoff frequency of the ac-coupled baseband, as shown in Fig. 12(c). The less radian difference means the closer the trajectory length without and with DPoD. The demodulated displacement without DPoD is 11.1 mm, which is 0.9 mm away from the ground truth of 12 mm, and the displacement with DPoD is 11.9 mm that has 0.1-mm error compared to the ground truth, as shown in Fig. 14.

It should be noted that the dc-offset calibration algorithm plays an important role in conditioning the measured I/Q signals for phase demodulation. It eliminates the dc offsets, normalizes the amplitudes, and adjusts the location of the I/Q trajectory on the unit circle. The calibration algorithm utilizes the measured data to find the centroid for the I/Q trajectory [32]. For the distorted I/Q trajectory, the ribbon-like shape may lead different algorithms to generate different centroids and different trajectory radians, resulting in different demodulation results [32]. The proposed DPoD technique helps to eliminate the ribbon shape and effectively improve EVM. Therefore, the measured I/Q signals could form an ideal arch in the I/Q plane, which makes sure that different calibration algorithms could generate similar, if not the same, centroid for the same I/Q signals.

B. Exp. 2: Fast Mechanical Motion

It has been demonstrated that the proposed DPoD technique is effective to compensate the distortion that is due to the low motion frequency within the stopband of the ac-coupled baseband. In this experiment, the same radar sensor was used to measure a fast motion whose frequency is away beyond the baseband cutoff frequency of 0.32 Hz. As shown in Fig. 2, if the motion frequency is within the passband, it is expected
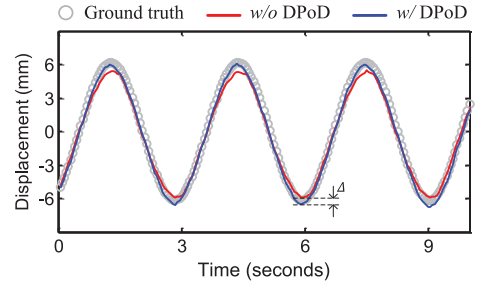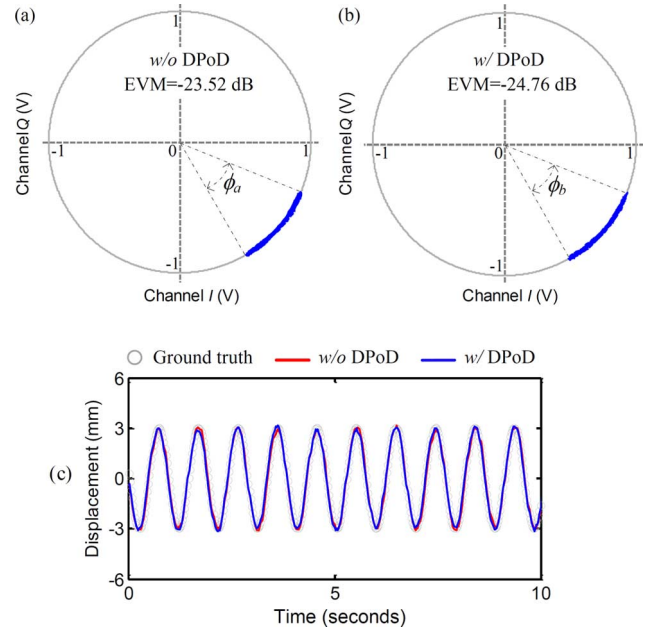

Fig. 15. I/Q trajectory of radar measured signals for a 1.05-Hz fast sinusoidal motion: (a) without DPoD and (b) with DPoD. (c) Demodulated displacement signal with and without DPoD is compared with the ground truth.

that the fundamental and the harmonics would suffer from very similar attenuation that is mainly the baseband insertion loss. Fig. 15 shows the experimental results for a fast motion with $m = 3$ mm and $f = 1.05$ Hz. It is seen in Fig. 15(a) that, without DPoD, the distorted ribbon shape no longer exits and the I/Q trajectory exhibits as an ideal arch sitting on the unit circle. It is because the fundamental-to-harmonics ratios are not distorted when the motion frequency is within the passband of the baseband high-pass filter. The DPoD response is flat in passband so that applying DPoD does not significantly affect the I/Q trajectory, but only improves EVM by 1.24 dB, as seen in Fig. 15(b). Empirical studies show that, as long as EVM is larger than 20 dB, further improved EVM does not help much to improve the demodulation accuracy for both the conventional arctangent demodulation [19] and the DACM demodulation [21]. There is little difference in the trajectory length without and with DPoD ($\phi_a = \phi_b$). The demodulated displacement without DPoD is 6.03 mm, which is almost the same as that with DPoD (5.98 mm), and both are matching well with the ground truth of 6.0 mm with high accuracy, as shown in Fig. 15(c). Therefore,

the proposed DPoD technique can be used in the signal-processing scheme for Doppler radar to measure motions with various speeds. It compensates the signal distortion for slow motions, but will not hurt the measurement accuracy for fast motions.

C. Exp. 3: Mechanical Motion With Stationary Moment

In Doppler motion sensing, if the subject stays still, the radar measured signal has no time-variant phase information, but constant phase shift, which means the radar output is the dc signal [15]. In order to keep the dc information, a dc-coupled radar sensor was proposed to measure the target motion that has stationary moment [15]. However, the dc-coupled radar requires complex dc tuning before it can measure the subject's motion. In this experiment, the simple ac-coupled radar was used to measure the subject's motion with stationary moment. The motion information programmed into the actuator was: a 3-s stationary moment, which was inserted between every two periods of a 0.3-Hz sinusoidal signal. The experimental results are illustrated in Fig. 16. Without DPoD, the distorted I/Q trajectory has an EVM of -13.9 dB. After applying DPoD, the I/Q trajectory fits better with the unit circle with an EVM of -22.02 dB, as shown in Fig. 16(b). Due to ac coupling at radar baseband, the information of the stationary moment was lost in the demodulated displacement signal, which can be seen in Fig. 16(c). The stationary moment is not the dc information from Bessel function $J_0(x)$ [35], which can be compensated in dc calibration [32]. As any periodic signal can be expanded as representation of Fourier series, the sinusoidal signal with stationary moment can also be represented by multiple single sinusoidal motions with different frequencies. That being said, the stationary moment is determined by the summation of harmonics. The high-pass characteristics of ac coupling distort the harmonic ratios, which lead to the loss of the information of the stationary moment. The DPoD technique is able to remedy the harmonic ratios to restore the stationary moment. As shown in Fig. 16(d), the recovered signal has the stationary moment recovered and matches very well with the ground truth.

The used DPoD coefficients were calibrated as $b_1 = 1$ and $a_1 = 0.955$. Fig. 16 shows the demodulated displacement signals using different DPoD coefficients. As shown in Fig. 17(a), when $a_1 = 0.98$, the distortion is reduced as compared to that in Fig. 16(c). However, there is still discrepancy as compared to the ground truth. In this case, the DPoD compensation is not enough to compensate the whole distortion. In other words, it is "under-compensation." When $a_1 = 0.93$, the displacement signal is over-compensated, as shown in Fig. 17(b). The discrepancy stays above the ground truth, while it is below the ground truth in under-compensation. Over-compensation happens because the magnitude of the fundamental tone is "over-amplified" by DPoD. Calibration of the radar system to generate the accurate DPoD coefficients is critical in distortion compensation.

D. Exp. 4: Human Respiratory Motion

The typical signal pattern of respiratory motion for a healthy adult at rest includes a short period of stationary moment: the respiration tends to rest for a moment at the end of expiration
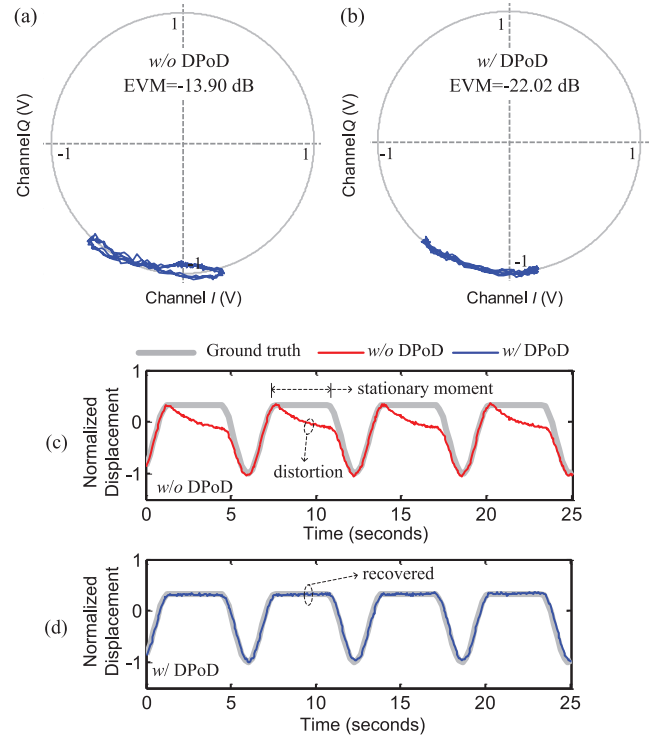

Fig. 16. I/Q trajectory of radar measured signals for a sinusoidal motion with stationary moment: (a) without DPoD and (b) with DPoD. The demodulated displacement signal without and with DPoD is compared with the ground truth: (c) without DPoD and (d) with DPoD.
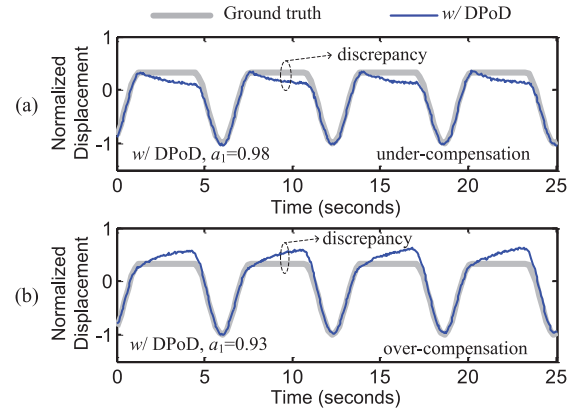

Fig. 17. Demodulated displacement signal for a sinusoidal motion with stationary moment using DPoD coefficients that deviate from the calibrated one: (a) $a_1 = 0.98$ and (b) $a_1 = 0.93$.

[15]. The same ac-coupled radar and the dc-coupled radar [25] were used to simultaneously measure the respiration of a subject person at rest. It has been demonstrated that the dc-coupled radar has high accuracy in motion detection [15] so that it is used as a reference. Fig. 18 shows the experimental results. It is seen from Fig. 18(a) that, without DPoD, the respiration signal measured by the ac-coupled radar shows distortion, which is similar to Exp. 3. The stationary moment is lost at the end of expiration. With DPoD, the stationary moment is recovered and the motion pattern matches well with the respiration measured by the dc-coupled radar, as shown in Fig. 18(b). Fig. 18(c) shows
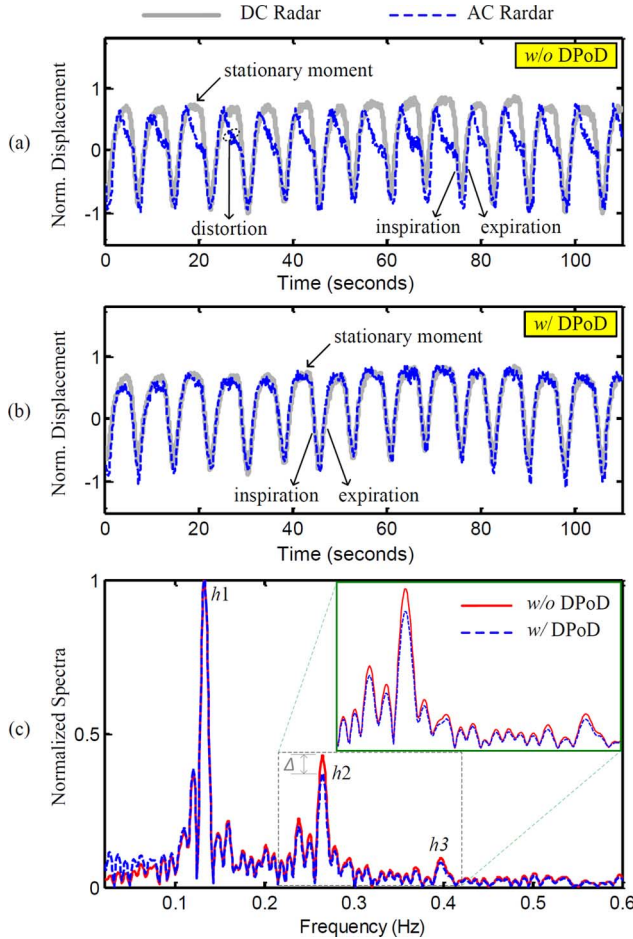
Fig. 18. Respiration motion measured by ac-coupled radar with/without DPoD is compared with that measured by dc-coupled radar: (a) without DPoD and (b) with DPoD. (c) Complex spectra of I/Q signals measured by ac-coupled radar with/without DPoD. Inset shows the zoom-in spectra near the second harmonic.

the spectral comparison of the ac-coupled radar measured respiratory motion without and with DPoD. It is shown that the spectrum is more complex than that of the sinusoidal motions in Figs. 11 and 13. It is because the breathing activity is not always constant over time, but may have varying magnitude and frequency. For example, a subject may take a deep breath at times. The inset in Fig. 18(c) shows the zoom-in spectra near the second harmonic of the respiratory signal. The DPoD technique is able to compensate the distortion to the spectral components to recover the complete signal pattern for the respiratory motion. Without adding any hardware complexity, the proposed DPoD technique allows the conventional Doppler radar with a simple ac-coupled structure to be able to measure the complete respiration pattern without losing significant information.

V. Conclusion

Signal distortion may happen in the conventional ac-coupled radar system using quadrature direct-conversion architecture. A DPoD technique has been proposed to compensate signal distortion in the baseband digital domain. Without any hardware modification or adding extra cost to the simple quadrature direct-conversion architecture, the proposed DPoD technique allows the ac-coupled radar to measure periodic motions without losing key information on motion pattern. Experiments have

shown that the DPoD technique could be used in measuring versatile periodic motions with high accuracy.

References

[1] J. C. Lin, "Noninvasive microwave measurement of respiration," *Proc. IEEE*, vol. 63, no. 10, pp. 1530–1530, Oct. 1975.

[2] M. Mercuri *et al.*, "Analysis of an indoor biomedical radar-based system for health monitoring," *IEEE Trans. Microw. Theory Techn.*, vol. 61, no. 5, pp. 2061–2068, May 2013.

[3] V. M. Lubecke, O. Boric-Lubecke, A. Host-Madsen, and A. E. Fathy, "Through-the-wall radar life detection and monitoring," in *IEEE MTT-S Int. Microw. Symp. Dig.*, Jun. 2007, pp. 769–772.

[4] C. S. Lin, S. F. Chang, C. C. Chang, and C. C. Lin, "Micro wave human vocal vibration signal detection based on Doppler radar technology," *IEEE Trans. Microw. Theory Techn.*, vol. 58, no. 8, pp. 2299–2306, Aug. 2010.

[5] T. Jaeschke, C. Bredendiek, S. Kuppers, and N. Pohl, "High-precision D-band FMCW-radar sensor based on a wideband SiGe-transceiver MMIC," *IEEE Trans. Microw. Theory Techn.*, vol. 62, no. 12, pp. 3582–3597, Dec. 2014.

[6] F.-K. Wang, T.-S. Horng, K.-C. Peng, J.-K. Jau, J.-Y. Li, and C.-C. Chen, "Single-antenna Doppler radars using self and mutual injection locking for vital sign detection with random body movement cancellation," *IEEE Trans. Microw. Theory Techn.*, vol. 59, no. 12, pp. 3577–3587, Dec. 2011.

[7] S. Mann, F. Lurz, R. Weigel, and A. Koelpin, "A high-sensitivity radar system featuring low weight and power consumption," *IEEE Microw. Mag.*, vol. 16, no. 2, pp. 99–105, Mar. 2015.

[8] T. Kao, Y. Yan, T. Shen, A. Chen, and J. Lin, "Design and analysis of a 60-GHz CMOS Doppler micro-radar system-in-package for vital-sign and vibration detection," *IEEE Trans. Microw. Theory Techn.*, vol. 61, no. 4, pp. 1649–1659, Apr. 2013.

[9] C. Gu, T. Inoue, and C. Li, "Analysis and experiment on the modulation sensitivity of Doppler radar vibration measurement," *IEEE Microw. Wireless Compon. Lett.*, vol. 23, no. 10, pp. 566–568, Oct. 2013.

[10] M. Pieraccini, M. Fratini, F. Parrini, and C. Atzeni, "Dynamic monitoring of bridges using a high-speed coherent radar," *IEEE Trans. Geosci. Remote Sens.*, vol. 44, no. 11, pp. 3284–3288, Nov. 2006.

[11] K.-M. Chen, Y. Huang, J. Zhang, and A. Norman, "Microwave life-detection systems for searching human subjects under earthquake rubble or behind barrier," *IEEE Trans. Biomed. Eng.*, vol. 27, no. 1, pp. 105–114, Jan. 2000.

[12] C. Li, J. Cummings, J. Lam, E. Graves, and W. Wu, "Radar remote monitoring of vital signs," *IEEE Microw. Mag.*, vol. 10, no. 1, pp. 47–56, Feb. 2009.

[13] W. Massagram, V. M. Lubecke, and O. Boric-Lubecke, "Microwave non-invasive sensing of respiratory tidal volume," in *Proc. Annu. IEEE Int. Eng. Med. Biol. Soc. Conf.*, 2009, pp. 4832–4835.

[14] M. Kagawa, K. Ueki, H. Tojima, and T. Matsui, "Noncontact screening system with two microwave radars for the diagnosis of sleep apnea-hypopnea syndrome," in *Proc. Annu. IEEE Int. Eng. Med. Biol. Soc. Conf.*, 2013, pp. 2052–2055.

[15] C. Gu, R. Li, H. Zhang, A. Fung, C. Torres, S. Jiang, and C. Li, "Accurate respiration measurement using DC-coupled continuous-wave radar sensor for motion-adaptive cancer radiotherapy," *IEEE Trans. Biomed. Eng.*, vol. 59, no. 11, pp. 3117–3123, Nov. 2012.

[16] S. Guan, J. A. Rice, C. Li, Y. Li, and G. Wang, "Dynamic and static structural displacement measurement using backscattering DC coupled radar," *Smart Struct. Syst.*, vol. 16, no. 3, pp. 521–535, 2015.

[17] C. Li, V. M. Lubecke, O. Boric-Lubecke, and J. Lin, "A review on recent advances in Doppler radar sensors for noncontact healthcare monitoring," *IEEE Trans. Microw. Theory Techn.*, vol. 61, no. 5, pp. 2046–2060, May 2013.

[18] A. D. Droitcour, O. Boric-Lubecke, V. M. Lubecke, J. Lin, and G. T. A. Kovacs, "Range correlation and I/Q performance benefits in single-chip silicon Doppler radars for noncontact cardiopulmonary monitoring," *IEEE Trans. Microw. Theory Techn.*, vol. 52, no. 3, pp. 838–848, Mar. 2004.

[19] B. K. Park, O. Boric-Lubecke, and V. M. Lubecke, "Arctangent demodulation with DC offset compensation in quadrature Doppler radar receiver systems," *IEEE Trans. Microw. Theory Techn.*, vol. 55, no. 5, pp. 1073–1079, May 2007.

[20] S. Kim and C. Nguyen, "A displacement measurement technique using millimeter-wave interferometry," *IEEE Trans. Microw. Theory Techn.*, vol. 51, no. 6, pp. 1724–1728, Jun. 2003.

This article has been accepted for inclusion in a future issue of this journal. Content is final as presented, with the exception of pagination.

GU *et al.*: HIGH-PRECISION MOTION DETECTION USING LOW-COMPLEXITY DOPPLER RADAR WITH DPoD TECHNIQUE 11

[21] J. Wang, X. Wang, L. Chen, J. Huangfu, C. Li, and L. Ran, "Non-contact distance and amplitude independent vibration measurement based on an extended DACM algorithm," *IEEE Trans. Instrum. Meas.*, vol. 63, no. 1, pp. 145–153, Jan. 2014.

[22] C. Gu *et al.*, "Noncontact large-scale displacement tracking: Doppler radar for water level gauging," *IEEE Microw. Wireless Compon. Lett.*, vol. 24, no. 12, pp. 899–901, Dec. 2014.

[23] A. Singh *et al.*, "Data-based quadrature imbalance compensation for a CW Doppler radar system," *IEEE Trans. Microw. Theory Techn.*, vol. 61, no. 4, pp. 1718–1724, Apr. 2013.

[24] M. Zakrzewski *et al.*, "Quadrature imbalance compensation with ellipse-fitting methods for microwave radar physiological sensing," *IEEE Trans. Microw. Theory Techn.*, vol. 62, no. 6, pp. 1400–1408, Jun. 2013.

[25] C. Gu and C. Li, "DC coupled CW radar sensor using fine-tuning adaptive feedback loop," *IET Electron. Lett.*, vol. 48, no. 6, pp. 344–345, Mar. 2012.

[26] R. Merched, "Roles of equalization in radar imaging: Modeling for superesolution in 3D reconstruction," *EURASIP J. Adv. Signal Process.*, vol. 2012, May 2012, 18 pp.

[27] R. Chavanne, K. Abed-Meraim, and D. Medynski, "Target detection improvement using blind channel equalization OTHR communication," in *Proc. Sens. Array Multichannel Signal Process. Workshop*, Jul. 18–21, 2004, pp. 657–661.

[28] W. R. McGrath, "Remote sensing method and device," U.S. Patent 7,811,234 B2, Sep. 18, 2007.

[29] C. Gu and C. Li, "Frequency-selective distortion in continuous-wave radar displacement sensor," *IET Electron. Lett.*, vol. 48, no. 23, pp. 1495–1497, 2012.

[30] I. Mostafanezhad, O. Boric-Lubecke, and V. Lubecke, "A coherent low IF receiver architecture for Doppler radar motion detector used in life signs monitoring," in *IEEE Radio Wireless Symp.*, 2010, pp. 571–574.

[31] C. Gu, C. Li, J. Huangfu, J. Lin, and L. Ran, "Instrument-based non-contact Doppler radar vital sign detection system using heterodyne digital quadrature demodulation architecture," *IEEE Trans. Instrum. Meas.*, vol. 59, no. 6, pp. 1580–1588, Jun. 2010.

[32] S. Guan, J. A. Rice, C. Li, and C. Gu, "Automated DC offset calibration strategy for structural health monitoring based on portable CW radar sensor," *IEEE Trans. Instrum. Meas.*, vol. 63, no. 12, pp. 3111–3118, Dec. 2014.

[33] C. Gu, G. Wang, T. Inoue, and C. Li, "A hybrid radar-camera sensing system with phase compensation for random body movement cancellation in Doppler vital sign detection," *IEEE Trans. Microw. Theory Techn.*, vol. 61, no. 12, pp. 4678–4688, Dec. 2013.

[34] W. Xu, C. Gu, C. Li, and M. Sarrafzadeh, "Robust Doppler radar demodulation via compressed sensing," *IET Electron. Lett.*, vol. 48, no. 22, pp. 1428–1430, 2012.

[35] C. Li, Y. Xiao, and J. Lin, "Experiment and spectral analysis of a low-power Ka-band heartbeat detector measuring from four sides of a human body," *IEEE Trans. Microw. Theory Techn.*, vol. 54, no. 12, pp. 4464–4471, Dec. 2006.

Changzhan Gu (S'07–M'13) received the B.S. and M.S. degrees in electrical engineering from Zhejiang University, Hangzhou, China, in 2006 and 2008, respectively, the M.S. degree in electrical engineering from the University of Florida, Gainesville, FL, USA, in 2010, and the Ph.D. degree in electrical engineering from Texas Tech University, Lubbock, TX, USA, in 2013.

He is currently a Member of the Technical Research Team of Project Soli with the Advanced Projects and Technology (ATAP) Group, Google, Mountain View, CA, USA. Prior to that, he was with Marvell Semiconductor Inc., where he was involved with wireless connectivity system-on-chip (SoC), and MaxLinear Inc., where he was involved with satellite TV tuner SoCs. His research interests include RF and microwave circuits/systems, RF SoCs, wireless sensing technologies, and the biomedical applications of RF/microwave.

Dr. Gu was the recipient of seven IEEE-sponsored conferences Best Paper Awards as an author/coauthor. He was the recipient of the 2013 IEEE Microwave Theory and Techniques Society (MTT-S) Graduate Fellowship for Medical Applications, the 2013 Texas Tech Horn Professors Graduate Achievement Award, and the 2012 Chinese Government Award for Outstanding Self-Financed Students Abroad.

Zhengyu Peng (S'15) received the B.S. and M.Sc. degrees in electrical engineering from Zhejiang University, Hangzhou, China, in 2011 and 2014, respectively, and is currently working toward the Ph.D. degree in electrical engineering at Texas Tech University (TTU), Lubbock, TX, USA.

His research interests include antennas, microwave circuits, and biomedical applications of microwave/RF circuits and systems.

Changzhi Li (S'06–M'09–SM'13) received the B.S. degree in electrical engineering from Zhejiang University, Hangzhou, China, in 2004, and the Ph.D. degree in electrical engineering from the University of Florida, Gainesville, FL, USA, in 2009.

During the summers of 2007–2009, he was with Alereon inc. Austin, TX, USA, and Coherent Logix Inc. Austin, TX, USA, where he was involved with ultra-wideband (UWB) transceivers and software-defined radio. In 2009, he joined Texas Tech University, Lubbock, TX, USA, as an Assistant Professor, and in 2014 became an Associate Professor. His research interests include biomedical applications of microwave/RF, wireless sensors, and analog circuits.

Dr. Li is an Associate Editor for the IEEE TRANSACTIONS ON CIRCUITS AND SYSTEMS—I: REGULAR PAPERS. He served as the Technical Program Committee (TPC) co-chair for the IEEE Wireless and Microwave Technology Conference (WAMICON) in 2012 and 2013. He was the recipient of the ASEE Frederick Emmons Terman Award in 2014, the IEEE HKN Outstanding Young Professional Award in 2014, the National Science Foundation (NSF) Faculty Early CAREER Award in 2013, and the IEEE Microwave Theory and Techniques Society (IEEE MTT-S) Graduate Fellowship Award in 2008. He was also the recipient of nine Best Conference/Student Paper Awards as an author/advisor at IEEE-sponsored conferences.